Hydrol. Earth Syst. Sci. Discuss., 10, 12417–12451, 2013
www.hydrol-earth-syst-sci-discuss.net/10/12417/2013/
doi:10.5194/hessd-10-12417-2013

Hydrology and Earth System Sciences
Discussions
Open Access

Climate change, vegetation restoration and engineering as a 1 : 2 : 1 explanation for reduction of suspended sediment in southwest China

X. Ma[1,2,3], X. Lu[4], M. van Noordwijk[5], J. Xu[1,2], and J. Li[6]

[1]Center for Mountain Ecosystem Studies, Kunming Institute of Botany, Kunming, 650204 China
[2]World Agroforestry Centre, Kunming Office, Kunming, 650204 China
[3]Yunnan Institute of Environmental Sciences, Kunming, 650034 China
[4]Department of Geography, National University of Singapore, 117570 Singapore
[5]World Agroforestry Centre, Southeast Asia, Bogor 16001, Indonesia
[6]Baoshan Water Resource and Hydrological Bureau, Baoshan, 678000 China

Received: 19 August 2013 – Accepted: 26 September 2013 – Published: 15 October 2013

Correspondence to: J. Xu (j.c.xu@cgiar.org)

Published by Copernicus Publications on behalf of the European Geosciences Union.

Abstract

Suspended sediment transport in rivers is controlled by terrain, climate and human activities. These variables affect hillslope and riverbank erosion at the source, transport velocities and sedimentation opportunities in the river channel, and entrapment in reservoirs. The relative importance of those factors varies with context but correct attribution is important for policy debates. We analyzed data from the Kejie watershed in the upper Salween, where a combination of land cover change (reforestation, soil and water conservation measures) and river channel engineering (sand mining and check dam construction) interact with a changing climate. Long-term records (1971–2010) of river flow and suspended sediment loads were combined with five land use maps from 1974, 1991, 2001, 2006 and 2009. Average annual sediment yield decreased from 13.7 $t\,ha^{-1}\,yr^{-1}$ to 8.3 $t\,ha^{-1}\,yr^{-1}$ between the 1971–1985 and 1986–2010. A distributed hydrological model (Soil and Water Assessment Tools, SWAT) was set up to simulate the sediment sourcing and transport process. By recombining land use and climate data for the two periods in model scenarios, the contribution of these two factors could be assessed with engineering effects derived from residual measured *minus* modeled transport. Overall 46 % of the decrease was due to from land use and land cover change, 25 % to climate change to a milder rainfall regime, 25 % to engineering measures, and 4 % to simulation bias. Mean annual suspended sediment yield decreased exponentially with the increase of forest cover. We discuss the implications for future soil and water conservation initiatives in China.

1 Introduction

Sediment transport in rivers can be a symptom of erosion problems, but it also increases with landslides, riverbank instability, and disturbances such as (road) construction and mining activities. Dam construction negatively impacts the level (Verbist et al., 2010). Walling and Fang (2003) found that among 145 rivers in a global dataset

HESSD

10, 12417–12451, 2013

Reduction of suspended sediment in southwest China

X. Ma et al.

on annual sediment loads, 4.8 % (7 rivers) had an increased load, 49.3 % (70 rivers) were stable and 46.9 % (68 rivers) had a decreased load. Liu et al. (2008) similarly classified the 10 major rivers in China and found seven with decreasing sediment and stable runoff, one with decreasing sediment and runoff, and two with significant decreases in sediment and runoff. Dai et al. (2009) reported that the decadal suspended sediment flux decreased by 70.2 % from 1.81 Gt yr^{-1} for 1954–1963 to 0.54 Gt yr^{-1} for 1996–2005 in nine major rivers in China.

Soil erosion is caused by the interaction between climate (especially rainfall intensity, amount and distribution), terrain properties and human activities (Dai et al., 2009), and results in a major loss of natural capital (Pimentel, 2006). Vegetation restoration (i.e. tree planting, grass establishment and ecological restoration measures) and engineering measures (i.e. terrace and silt check dams) are commonly employed for erosion control in China (Huang and Zhang, 2004). The relative contribution of these measures is a debated issue and may depend on local context.

Check dams were identified as the most effective short-term measure for reducing coarse sediment entering the Yellow River riverbank (Ran et al., 2008; Xiang-Zhou et al., 2004; Xu et al., 2013). Reservoirs intercept most of the suspended sediments and override any effect of erosion reduction (Rijsberman and Wolman, 1985). Over the past 20 yr, vegetation-based soil and water conservation has had a negligible effect on the Pearl River (Wu et al., 2012), contributing only 9.2 % to reduction of sediment load in the Miyun reservoir, Beijing (Tang et al., 2011); and less than 15 % reduction to the Three Gorges Reservoir (Ming et al., 2009) and Yangtze River (Dai et al., 2008). However, Wang et al. (2007b) found that soil conservation measures were responsible for 40 % to the total sediment load decrease in the Yellow River basin. The relationship between forest cover and soil erosion is complex (Ran et al., 2013) as the litter layer and understory vegetation, which exert primary control, varies with forest, vegetation type and management (Hairiah et al., 2006). Mixed forest may be the most effective for controlling erosion (Men, 2011). But none of these studies have considered the impacts of climatic variation and change, which likely interact with the roles of vegetation.

According to soil conservation zone planning, the Kejie watershed is a key protection area in Yunnan province. In light of the alternative solutions for controlling sediment loading in streams, it is important to understand the role of the vegetation restoration and engineering measures previously undertaken for erosion control. In recent decades there has been little change in average annual runoff but a dramatic decrease in annual sediment yield. As there is currently no widely accepted method for attributing the decline of sediment yield to land use and land cover change, engineering efforts and climate change, we set out to explore a modeling approach in which land cover effects, climate and engineering impacts can be separated by recombination.

The objective of this article is to use the data available for the Kejie watershed to (1) detect the change trend of suspend sediment yield at the outlet of the watershed; (2) explore the potential driving factors that led to the decrease of suspended sediment load in the watershed; (3) quantify the contribution of vegetation restoration to the decrease in sediment load, using a distributed hydrological model (SWAT) based on five time periods land use maps; (4) quantify the relationship between forest cover and soil erosion modulus in the watershed; (5) tease out the climate effect by switching rainfall records and (6) identify the effects of engineering based on the difference between modeled (in the absence of engineering) and measured sediment loads.

2 Description of the watershed

The Kejie watershed in western Yunnan Province is an upstream watershed in the Salween Basin and has a total area of 1755 km^2 (Fig. 1). The Donghe River, a major tributary of the upper Salween River, is the main watercourse and runs for 95.2 km with an average slope of 11^0 (ranging from 1 to 88^0). The watershed provides environmental goods and services to Baoshan Prefecture in Yunnan and to Myanmar and Thailand downstream. The climate is sub-tropical in the valley and temperate in mountain areas. The mean annual precipitation is 994.5 mm with a recorded maximum of 1368.3 mm in 2001 and minimum of 663.3 mm in 2009. More than 80 % of the precipitation occurs in the monsoon season from May to October. Annual runoff varies between $3.3 \times 10^8\,m^3$ (2005) and $11.0 \times 10^8\,m^3$ (2001) with an average of $6.4 \times 10^8\,m^3$. Effective water yield is (188)-364-(627) $mm\,yr^{-1}$. River flow data were analyzed by Ma et al. (2009a).

Administratively, the Kejie watershed covers most of Longyang County and small parts of Shidian and Changning County, all in the Baoshan Prefecture. Baoshan is considered to be a key watershed protection area (Fig. 1b). While 34.2 % of the total area in Yunnan province is classified as sensitive to soil erosion, 37 % of Baoshan prefecture, and 49 % of Longyang county were classified as such in 2004 (Ma et al., 2009b). Of the total erosion-sensitive area in Longyang County, 76.8 % was classified as medium erosion prone, 18.5 % as slightly erosion prone, and 4.7 % as high-risk erosion area. Landslides and small-scale mud-rock flows happen frequently, with heavy damages to property. Great efforts have been made by the central and local government in China to combat soil erosion since 1980's.

In recent decades, annual sediment yield has varied between 14.7×10^4 t (2005; $0.84\,t\,ha^{-1}\,yr^{-1}$) and 495.1×10^4 t (1985; $28.2\,t\,ha^{-1}\,yr^{-1}$) with an average of 173.0×10^4 t ($9.86\,t\,ha^{-1}\,yr^{-1}$). The main soil type is red. The natural vegetation of semi-moist broadleaved forest disappeared many decades ago and has been replaced by conifer with a mix of alder (*Alnus nepalensis*) and other broadleaved species.

There is a middle-sized reservoir with a capacity of $5.850 \times 10^4\,m^3$, namely Beimiaoshuiku (BSK), located in up-stream Donghe River, which was built in 1958 and has been operational since 1959 (Fig. 1c). As the reservoir was operational before the start of our study period (1965) and its management has not undergone major change, its main effect in this study was as a constant sediment trap for its upstream area.

HESSD
10, 12417–12451, 2013

3 Materials and methods

3.1 Available materials

3.1.1 Hydro-meteorological datasets

Three meteorological stations with long-term records (1965–2010) in or adjacent to the Kejie watershed, and one with short-term records (1998–2002) in the Xizhuang sub-watershed, were available. The daily value of six parameters were collected, namely rainfall, maximum temperature, minimum temperature, wind speed, relative humidity, and sunshine hours. In addition, two rainfall stations with long-term daily rainfall data in the Kejie watershed (1965–2010), and seven rainfall stations with short-term daily rainfall data in the Xizhuang sub-watershed (1998–2002), were available. One hydrological station with long-term daily discharge and suspended sediment data is located at the outlet of the Kejie watershed (1965–2010). One middle-size reservoir with long-term daily outflow readings is situated in the upper reaches of the Donghe River in the Kejie watershed (1965–2010). All hydro-meteorological datasets were provided by the Baoshan Department of Hydrology and Meteorology (Fig. 1c, Table 1).

3.1.2 Land use maps

The soil map, digital elevation model (DEM) and vegetation/crop parameters were discussed by Ma et al. (2009a). Five land use maps of the Kejie watershed were used to analyze land use change in the past decades. Maps for 1974, 1991, 2001 and 2006 were classified by Ma et al. (2009a); an additional map for 2009 was obtained from the Baoshan Department of Forestry, based on a SPOT 5 image from 2009. As the classification of this 2009 map was more detailed than the previous maps, map units were combined to match the earlier legend.

HESSD
10, 12417–12451, 2013

3.2 Change trend detection

The areal annual rainfall was calculated on the basis of annual rainfall from five rainfall stations with long-term observed data using the Inverse Distance Weighted (IDW) method of ESRI ArcGIS9.3. The annual runoff and SSY was summarized on the basis of the daily values from the outlet of the Kejie watershed.

A non-parametric test, a Mann–Kendall test (Mann, 1945; Kendall, 1975) was performed alongside the parametric *t*-test in the monotonic change trend detection for long-term records (van Belle and Hughes, 1984); this has been extensively used with environmental time series (Burn et al., 2004; Ma et al., 2009a). Here we used it to identify the trend of annual rainfall, rainfall erosivity (R-factor), runoff and SSY. Tests used the Kendall package in the R statistical analysis software (Team, 2008).

Piecewise-regression model is an effective tool to model abrupt thresholds. In a "broken-stick" model, two or more lines are joined at unknown point(s), called "breakpoint(s)" (Toms and Lesperance, 2003) and are widely used to identify ecological thresholds (Oswald et al., 2011; Zhang et al., 2013). A simple model with two straight lines joined sharply at the breakpoint, appropriate when there is an abrupt transition, was selected in this study and implemented in R (Team, 2008), with the following equations:

$$y_i = \begin{cases} \beta_0 + \beta_1 t_i + \varepsilon, & t \le \alpha \\ \beta_0 + \beta_1 t_i + \beta_2 (t_i - \alpha)\varepsilon, & t > \alpha \end{cases} \quad (1)$$

Where y_1 is the annual suspended sediment yield, t_i is the corresponding year, α is the turn-point (year), and β_0, β_1 and β_2 are regression coefficients. ε is the residual of the fit. Before the turning point the slope of the line is β_1, afterwards it is $\beta_1 + \beta_2$.

3.3 Model selection and description

We used the SWAT model calibrated and validated with the Kejie watershed water balanced data (Ma et al., 2009a) from 1971 to 1979 to simulate the suspended sediment yield (SSY) under 5 different land use maps. The SWAT model, predicting long-term impacts of land use on water, sediment and agricultural chemical yield in large complex watersheds with varying soils, land-use and management conditions (Arnold and Fohrer, 2005), is widely used to simulate the SSY (Betrie et al., 2011; Cai et al., 2012; Oeurng et al., 2011; Qiu et al., 2012). For erosion, it uses the Modified Universal Soil Loss Equation (MUSLE) developed by Williams and Berndt (Williams and Berndt, 1977).

In SWAT, a watershed is divided into multiple sub-basins, which are further subdivided into Hydrologic Response Units (HRU) consisting of uniform land-cover, soil, and slope that drain directly to the sub-basin's channel. The hydrological modeling component in SWAT was discussed in Ma et al. (2009a). Details of MUSLE equation factors can be found in Neitsch et al. (2011). The channel sediment routing equation uses a modification of Bagnold's sediment transport equation (Bagnold, 1977). Sediment deposition in the channel is based on stream power (Williams, 1980) and fall velocity related to particle size. Channel degradation is adjusted using USLE soil erodibility and channel cover factors (Arnold et al., 1995).

Calibration of sediment yield was carried out manually through trial and error until satisfactory results were obtained. Based on previous studies (Betrie et al., 2011; Cai et al., 2012; Oeurng et al., 2011; Qiu et al., 2012), nine parameters are often considered when simulating sediment yield in SWAT, namely USLE-C (land cover factor in USLE equation), USLE_P (practice factor in USLE equation), SPCO (linear parameter for calculating the maximum amount of sediment that can be re-entrained during channel sediment routing), SPEXP (Exponent parameter for calculating sediment re-entrained in channel sediment routing), PRF (peak rate adjustment factor for sediment routing in the main channel), CH_COV (Channel cover factor), CH_Erod (channel erodibility factor), ADJ_PKR (peak rate adjustment factor for sediment routing in sub-basin).

3.4 Model setup and evaluation

The ArcSWAT model version 2009.93.7b was run in an ArcGIS 9.3 interface, with basic parameters as described by Ma et al. (2009a). Because observed sediment data was not complete in 1967, and the data in 1970 was missing, the simulation period of 1965–1970 was treated as a "warming up" period for the model. Monthly SSY records from 1971–1980 were split into two segments, 1971–1975 and 1976–1980, in order to calibrate and subsequently validate sediment-relative parameters.

In term of evaluation of the performance of the model, three indexes were used, as before, the NSE (Nash–Sutcliff efficiency), PBIAS (percentage bias), and RSR (ratio of the root mean square error to the standard deviation of measured data) (Moriasi et al., 2007). Details can be found in Ma et al. (2009a).

3.5 Recombining climate change and land cover change

The calibrated and validated model was used to distinguish the effect of climate change, vegetation change and engineering measures on suspended sediment yield, by recombining climate and land cover data (Tang et al., 2011; Ma et al., 2009b). The effect of change in engineering measures was estimated from the difference between the observed and simulated SSY.

4 Results and discussion

4.1 Changing trends of suspended sediment yield

Annual rainfall, R-factor, runoff and Suspended sediment yield (SSY) all showed a declining trend (Fig. 2). The strongest, and only statistically significant, decrease was in SSY ($\alpha = 0.05$) (Table 2).

HESSD
10, 12417–12451, 2013

Per decade the SSY was related to annual runoff, but the relationship as a whole shifted (Fig. 3). When compared at any given runoff rate, annual SSY increased from 1970's to 1980's and subsequently declined.

A piecewise-regression model identified the breakpoint in recorded annual SSY to be 1985 (Fig. 4). Over the period 1971–1985, an increase was observed with a correlation coefficient of 0.29, which was not statistically significant (at $\alpha = 0.05$); there was a decrease from 1986–2010 and a statistically significant correlation coefficient of 0.80 ($\alpha = 0.05$) was recorded. A similar pattern of sediment yield change was observed at Yichang station, Yangtze River (Dai et al., 2009).

Since 1970s, many hillsides with vegetation had been converted to terraced fields to meet the food needs of an increasing population (Zhang et al., 1999). Road construction and other infrastructure development exacerbated soil erosion during this period. In the 1980's China made a transition from a central planning economy to a market economy. Measures were taken to rectify this issue; steep slopes were reforested and soil and water conservation programs including ecological restoration, were rolled out. Engineering measures (terrace improvement, silt check dam) also contributed to the decrease of sediment yield in the watershed. Other human activities, i.e. sand mining in the river (extraction of riverbed sediment) and riverbank protection, may have contributed to the decrease in sediment yield.

Using the breakpoint identified, the study period was divided into two periods: 1971–1985 (1) and 1986–2010 (2). From period 1 to 2, the mean annual rainfall, R-factor and runoff decreased by 3.8 %, 5.5 % and 10.8 % respectively, and mean annual SSY decreased by 39.7 %. The magnitudes of change in runoff and sediment were influenced by climate change, vegetation measures and other soil and water conservation measures.

4.2 Driving factors analysis

4.2.1 Climate change

Ma et al. (2009a) described a monotonic increasing trend in the average annual temperature of 0.41 °C $(10\,\mathrm{yr})^{-1}$ for the period since 1965. According to Lu et al. (2010), a similar temperature increase caused glacier recession and permafrost degradation in the headwaters of the Himalayas and the Tibetan Plateau. This occurred alongside an increase in sediment loads. The elevation of the Kejie watershed ranges from 963–3076 m a.s.l. and there is some snow cover on the mountaintop, but no glacier or permafrost. The influence of temperature on water yield and associated suspended sediment is likely negligible.

While the observed declining trend in annual rainfall in the watershed over 1971–2010 was not statistically significant, inter-annual variability ranged from −32.4 % (2009) to 25.1 % (2001) (Fig. 5a). A similar change trend was observed in the annual R-factor, although this exhibited greater variability (−45.5 % (2009) to 41.3 % (2001)) (Fig. 5b). As it is a main driving factor of soil erosion, the high variability in annual R-factor causes high variability in the predicted soil erosion and assessments are required, at least, a decadal basis.

4.2.2 Land use and land cover change

Land-cover estimates for the five observation points are summarized in Table 3. The cover fractions of forest, cropland and settlement increased by 33.9, 5.0 and 2 % respectively, while the area of grassland and barren land declined by 24.6 and 15.9 % respectively from 1974 to 2009, with small variations in what was identified as open water.

The increase of forest in the Kejie watershed (from 21.9 to 55.8 %) can be directly attributed to the forest policy of the central government in China. Aerial seeding of reforestation started in 1987, and followed by two large-scale conservation programs,

HESSD
10, 12417–12451, 2013

namely the Natural Forest Protection Program (NFPP), and the Grain for Green project (GGP) (which was originally called the Sloping Land Conversion Program), were implemented in China in the past decade. The NFPP was introduced in 1998 to rehabilitate and develop natural forests (Zhang et al., 2000). GGP started in 1999 and it aimed to restore the landscape by paying farmers to plant trees rather than crops (Wang et al., 2007a). The forest cover in China as a whole increased from 16.6 to 18.2 % in 2005, and the goal is to reach 26 % by 2050 (Wang et al., 2007a). Yunnan province was the priority for NFPP and was also in the priority areas of GGP. In the Kejie watershed, the forest cover increased from 37.3 to 55.8 % between 2001 and 2009. The increase ratio of forest cover from 2001 to 2009 was higher than for the period of 1974–2001.

4.2.3 Soil and water conservation programs

The first soil and water conservation program in Yunnan Province started in 1989 as part of a National Key Soil Conservation Project supported by the central government of China (Wei et al., 2011). After that, several soil and water conservation programs were launched, such as the Yangtze River treatment project, the Pearl River treatment project and the Treasury bond projects supported by the central government (Ma et al., 2009b). Ecological measures and engineering measures have been undertaken in these programs. On the basis of the local inventory data, five soil and water conservation projects (ranging in area between 20.36 and 27.87 km^2) were implemented in the Kejie watershed from 2000 to 2005. On the basis of the local inventory data, soil erosion area was reduced by 40–81 % (Fig. 6). Table 4 lists the contribution to the soil loss reduction from different measures. Generally speaking, the contribution from ecological measures was around 50 %. The value was with high uncertainty as the assessment method was somewhat subjective, and lacked details of the routing processes of sediment from the plot to watershed level.

4.2.4 Other human activities happened in the watershed

Soil erosion control measures taken in the process of the new constructing projects: Several construction projects were implemented in the watershed during the previous decades, which lead to soil wasting (Table 5). From 2004 to 2010, a total of $1907.3 \times 10^4\,m^3$ waste soil from construction sites was treated properly, as a key measure to prevent soil and water losses.

Sand mining near the riverbank: Several sand mining plants take sand from the Donghe River. It was difficult to quantify the amount of sand taken as the plants lacked a license and operated irregularly.

Riverbank protection: In order to prevent and eliminate the flood disaster, the riverbanks of the Donghe in the upper-stream were reconstructed with concrete during the past decades. These engineering measures could not be directly represented in the SWAT modeling.

4.3 Model calibration and validation

The watershed was divided into 45 sub-basins while the number of HRUs varied depending on the land cover map (353 for the 1974 map) in the SWAT model. The calibration attempts showed that the most sensitive parameters for sediment modeling in the Kejie watershed were USLE_P, SPCON, ADJ_PKR and CH_EROD. These parameters were adjusted from the initial estimates to fit the model simulations with the observed monthly sediment data over 1971–1975 (Fig. 7a).The calibrated parameters were validated from 1976 to 1980 (Fig. 7b). The calibrated values of the parameters are listed in Table 6. NSE, RSR and PBIAS indicators were 0.73, 0.52, and −4.6 % respectively. For the validation period, the simulated and observed monthly values resulted in a satisfactory model with NSE, RSR and PBIAS 0.77, 0.48, and −9.3 %, respectively. The model slightly under estimated the monthly suspended sediment. According to the criteria suggested by Moriasi et al. (2007), the performance of sediment simulation ranged from good to very good.

HESSD
10, 12417–12451, 2013

4.4 Partitioning observed change across climate and land cover change, and other engineering measures

The observed change (Measured2 – Measured1) was partitioned using simulation results for various combinations of land cover (L) and climate (C) as follows:

$$
\begin{aligned}
\text{Change} &= \text{Measured2} - \text{Measured1} \\
&= (\text{Measured2} - \text{SimulatedL2C2}) + (\text{SimulatedL2C2} - \text{SimulatedL1C2}) \\
&\quad + (\text{SimulatedL1C2} - \text{SimulatedL1C1}) + (\text{SimulatedL1C1} - \text{Measured1}) \\
&= [\text{Land use change effect}] + [\text{Climate change effect}] + [\text{Engineering effects}] \\
&\quad + [\text{Model bias}]
\end{aligned}
$$

The 1974 land-cover map was deemed to represent the land condition for the period 1970–1985; the 1991 land-cover map stood for 1986–1998, the 2001 map stood for 1999–2002, and the 2009 map stood for 2008–2010. Three scenarios were defined to represent different combinations of land use and climate condition, namely SimulatedL1C1, SimulatedL1C2 and SimulatedL2C2. SimulatedL1C1 was the baseline simulation for period1; SimulatedL1C2 was used to predict a "business as usual" scenario with the land cover kept constant into period 2; And SimulatedL2C2 was used to provide a counterfactual of what might happen in period 2 without engineering measures, but with actual land cover for 1986 to 2010. Table 7 lists the mean annual SSY over period1 and period2.

From period 1 to 2, the mean annual SSY decreased by 40 % ($95.6 \times 10^4\ \text{t yr}^{-1}$) under the joint impacts of human activities and climate change (Table 8); the value decreased by 10 % ($23.9 \times 10^4\ \text{t yr}^{-1}$) under the impact of climate change; the value decreased by 18 % ($44.1 \times 10^4\ \text{t yr}^{-1}$) under the impact of land cover change, and by 10 % ($23.8 \times 10^4\ \text{t yr}^{-1}$) under the impact of other engineering measures. The bias of the observed and simulated values was within 2 %, which indicated that the simulations were acceptable.

HESSD
10, 12417–12451, 2013

The decrease in the mean annual SSY from period 1 to 2 was 46 % attributable to land cover change, 25 % to climate change (a milder rainfall regime), and 25 % to other engineering measures. The bias from model simulation accounted for 4 % of the observed change (Table 8). Although the trend in rainfall is not statistically different from what can be expected for a no-change hypothesis, the predicted sediment yield is more sensitive to rainfall change than water discharge (Lu et al., 2013).

A comparison of the contributions of climate change and human activities (reforestation, ecological restoration measures, engineering measures, sand mining, and river-bank protection) showed that human activities were a governing factor for river sediment delivery, coinciding with the findings of Dai et al. (2009) in China. This work showed that reforestation and ecological restoration played a dominant role in controlling soil erosion.

4.5 Effect of ecological restoration on suspended sediment yield

To further explore the effect of vegetation restoration on SSY, 6 sub-basins with similar land cover and land use change trends were selected from the watershed (Fig. 8a). The total area was 421.8 km^2 with sub-basin size ranging from 35.8 km^2 to 133.1 km^2. The soil and water conservation programs described in Fig. 6 at the Ajiadahe, Binmawahe, Longwangmiao, Santaizihe and Wadudahe were located in sub-basin 1, 25, 2, 7, and 17 respectively. We assumed that the land cover in the watershed changed from the 1974 land use to the land use of 1991, 2001, 2006 and 2009 in the period 1 (1971–1985) respectively. The average annual soil erosion modulus (1971–1985) from six sub-basins under five land use maps was simulated using the calibrated and validated SWAT model. When the land cover changed from the 1974 map to the 2009 map, the reduction in the soil erosion modulus ranged between 15.56 and 34.58 $t\,ha^{-1}\,a^{-1}$ among 6 sub-basins. The relationship between the forest cover and soil erosion modulus is illustrated in Fig. 8b. An exponential relationship between the forest cover and soil erosion modulus represents the data adequately. The relationship implies reforestation and ecological restoration can effectively control soil erosion in these watersheds.

HESSD
10, 12417–12451, 2013

5 Conclusions

The data show a larger contribution of land use/cover change to the reduction in suspended sediment yield, relative to engineering and other human activities than the majority of previous studies elsewhere in China. The sharp decrease in sediment yield from 1985, although assisted by a milder rainfall regime, was mostly due to the effects of more than 10 yr of reforestation (forest cover increasing from 21.9 to 55.8 %) and soil and water conservation programs. Since 1985, the health and stability of the river ecosystem has significantly improved.

Acknowledgements. This research is part of the CGIAR Research Program 6: Forests, Trees and Agroforestry. We also would like to express our sincere gratitude to Baoshan Water Conservancy Bureau and Baoshan Meteorological Bureau for their data support.

References

Arnold, J. G. and Fohrer, N.: SWAT2000: current capabilities and research opportunities in applied watershed modelling, Hydrol. Process., 19, 563–572, doi:10.1002/hyp.5611, 2005.

Arnold, J. G., Williams, J., and Maidment, D.: Continuous-time water and sediment-routing model for large basins, J. Hydraul. Eng., 121, 171–183, doi:10.1061/(ASCE)0733-9429(1995)121:2(171), 1995.

Bagnold, R. A.: Bed load transport by natural rivers, Water Resour. Res., 13, 303–312, doi:10.1029/WR013i002p00303, 1977.

Betrie, G. D., Mohamed, Y. A., van Griensven, A., and Srinivasan, R.: Sediment management modelling in the Blue Nile Basin using SWAT model, Hydrol. Earth Syst. Sci., 15, 807–818, doi:10.5194/hess-15-807-2011, 2011.

Burn, D. H., Cunderlik, J. M., and Pietroniro, A.: Hydrological trends and variability in the Liard River basin/Tendances hydrologiques et variabilité dans le basin de la rivière Liard, Hydrol. Sci. J., 49, 53–67, doi:10.1623/hysj.49.1.53.53994, 2004.

Cai, T., Li, Q., Yu, M., Lu, G., Cheng, L., and Wei, X.: Investigation into the impacts of land-use change on sediment yield characteristics in the upper Huaihe River basin, China, Phys. Chem. Earth, 53–54, 1–9, doi:10.1016/j.pce.2011.08.023, 2012.

HESSD

10, 12417–12451, 2013

Reduction of suspended sediment in southwest China

X. Ma et al.

Dai, S. B., Lu, X. X., Yang, S. L., and Cai, A. M.: A preliminary estimate of human and natural contributions to the decline in sediment flux from the Yangtze River to the East China Sea, Quat. Int., 186, 43–54, doi:10.1016/j.quaint.2007.11.018, 2008.
Dai, S. B., Yang, S. L., and Li, M.: The sharp decrease in suspended sediment supply from China's rivers to the sea: anthropogenic and natural causes, Hydrol. Sci. J., 54, 135–146, doi:10.1623/hysj.54.1.135, 2009.
Hairiah, K., Sulistyani, H., Suprayogo, D., Widianto, Purnomosidhi, P., Widodo, R. H., and Van Noordwijk, M.: Litter layer residence time in forest and coffee agroforestry systems in Sumberjaya, West Lampung, For. Ecol. Manage., 224, 45–57, doi:10.1016/j.foreco.2005.12.007, 2006.
Huang, M. and Zhang, L.: Hydrological responses to conservation practices in a catchment of the Loess Plateau, China, Hydrol. Process., 18, 1885–1898, doi:10.1002/hyp.1454, 2004.
Kendall, M. G.: Rank correlation methods, Charles Griffin, London, UK, 1975.
Liu, C., Sui, J., and Wang, Z.-Y.: Sediment load reduction in Chinese rivers, Int. J. Sediment Res., 23, 44–55, doi:10.1016/S1001-6279(08)60004-9, 2008.
Lu, X. X., Zhang, S., and Xu, J.: Climate change and sediment flux from the Roof of the World, Earth Surf Process Landforms, 35, 732–735, doi:10.1002/esp.1924, 2010.
Lu, X. X., Ran, L. S., Liu, S., Jiang, T., Zhang, S. R., and Wang, J. J.: Sediment loads response to climate change: a preliminary study of eight large Chinese rivers, Int. J. Sediment Res., 28, 1–14, doi:10.1016/S1001-6279(13)60013-X, 2013.
Ma, X., Xu, J., Luo, Y., Prasad Aggarwal, S., and Li, J.: Response of hydrological processes to land-cover and climate changes in Kejie watershed, south-west China, Hydrol. Process., 23, 1179–1191, doi:10.1002/hyp.7233, 2009a.
Ma, X., Zhu, X., and Zhao, R.: Index system of DPSIR framework for soil erosion in Yunnan Province, Environmental Science Survey, 28, 1–5, 2009b (in Chinese with English abstract).
Mann, H. B.: Nonparametric tests against trend, Econometrica, 13, 245–259, 1945.
Men, G. T.: Treatment and benefit analysis on water and soil loss in Yunnan Province, China, Soil and Water Conservation in China, 2, 34–36, 2011(in Chinese with English abstract).
Ming, X., Quanxi, X., and Jing, Y.: Analysis of multi-factors affecting sediment load in the Three Gorges Reservoir, Quat. Int., 208, 76–84, 2009.
Moriasi, D., Arnold, J., Van Liew, M., Bingner, R., Harmel, R., and Veith, T.: Model evaluation guidelines for systematic quantification of accuracy in watershed simulations, Trans. ASAE, 50, 885–900, 2007.

Neitsch, S., Arnold, J., Kiniry, J., and Williams, J.: Soil and water assessment tool theoretical documentation: version 2009, Texas Water Resources Institute Technical Report 406, Texas A&M Univ, System, College Station, Texas, 2011.
Oeurng, C., Sauvage, S., and Sánchez-Pérez, J.-M.: Assessment of hydrology, sediment and particulate organic carbon yield in a large agricultural catchment using the SWAT model, J. Hydrol., 401, 145–153, 2011.
Oswald, C. J., Richardson, M. C., and Branfireun, B. A.: Water storage dynamics and runoff response of a boreal Shield headwater catchment, Hydrol. Process., 25, 3042–3060, doi:10.1002/hyp.8036, 2011.
Pimentel, D.: Soil erosion: a food and environmental threat, Environ. Dev. Sustainability, 8, 119–137, doi:10.1007/s10668-005-1262-8, 2006.
Qiu, L. J., Zheng, F. L., and Yin, R. S.: SWAT-based runoff and sediment simulation in a small watershed, the loessial hilly-gullied region of China: capabilities and challenges, Int. J. Sediment Res., 27, 226–234, doi:10.1016/S1001-6279(12)60030-4, 2012.
Ran, D. C., Luo, Q. H., Zhou, Z. H., Wang, G. Q., and Zhang, X. H.: Sediment retention by check dams in the Hekouzhen-Longmen Section of the Yellow River, Int. J. Sediment Res., 23, 159–166, doi:10.1016/S1001-6279(08)60015-3, 2008.
Ran, L., Lu, X., and Xu, J.: Effects of vegetation restoration on soil conservation and sediment loads in China: a critical review, Crit. Rev. Env. Sci. Tec., 43, 1384–1415, 2013.
Rijsberman, F. R. and Wolman, M. G.: Effect of erosion on soil productivity: an international comparison, J. Soil Water Conserv., 40, 349–354, 1985.
Tang, L., Yang, D., Hu, H., and Gao, B.: Detecting the effect of land-use change on streamflow, sediment and nutrient losses by distributed hydrological simulation, J. Hydrol., 409, 172–182, 2011.
Team, R. C.: R: A Language and Environment for Statistical Computing, Vienna, Austria, R Foundation for Statistical Computing, 1–1731, 2008.
Toms, J. D. and Lesperance, M. L.: Piecewise regression: a tool for identifying ecological thresholds, Ecology, 84, 2034–2041, 2003.
van Belle, G. and Hughes, J. P.: Nonparametric tests for trend in water quality, Water Resour. Res., 20, 127–136, doi:10.1029/WR020i001p00127, 1984.
Verbist, B., Poesen, J., van Noordwijk, M., Suprayogo, D., Agus, F., and Deckers, J.: Factors affecting soil loss at plot scale and sediment yield at catchment scale in a tropical volcanic agroforestry landscape, Catena, 80, 34–46, 2010.

Walling, D. and Fang, D.: Recent trends in the suspended sediment loads of the world's rivers, Global Planet. Change, 39, 111–126, 2003.
Wang, G., Innes, J. L., Lei, J., Dai, S., and Wu, S. W.: China's forestry reforms, Science, 318, 1556, 2007a.
Wang, H., Yang, Z., Saito, Y., Liu, J. P., Sun, X., and Wang, Y.: Stepwise decreases of the Huanghe (Yellow River) sediment load (1950–2005): impacts of climate change and human activities, Global Planet. Change, 57, 331–354, 2007b.
Wei, J., He, X., and Bao, Y.: Anthropogenic impacts on suspended sediment load in the Upper Yangtze river, Reg. Environ. Change, 11, 857–868, 2011.
Williams, J.: SPNM, a model for predicting sediment, phosphorous, and nitrogen yields from agricultural basin, J. Am. Water Resour. As., 16, 843–848, 1980.
Williams, J. and Berndt, H.: Sediment yield prediction based on watershed hydrology, Trans. ASAE, 20, 1100–1104, 1977.
Wu, C., Yang, S., and Lei, Y. P.: Quantifying the anthropogenic and climatic impacts on water discharge and sediment load in the Pearl River (Zhujiang), China (1954–2009), J. Hydrol., 452, 190–204, 2012.
Xiang-Zhou, X., Hong-Wu, Z., and Ouyang, Z.: Development of check-dam systems in gullies on the Loess Plateau, China, Environ. Sci. Policy, 7, 79–86, doi:10.1016/j.envsci.2003.12.002, 2004.
Xu, Y. D., Fu, B. J., and He, C. S.: Assessing the hydrological effect of the check dams in the Loess Plateau, China, by model simulations, Hydrol. Earth Syst. Sci., 17, 2185–2193, doi:10.5194/hess-17-2185-2013, 2013.
Zhang, G., Zhang, Y., Dong, J., and Xiao, X.: Green-up dates in the Tibetan Plateau have continuously advanced from 1982 to 2011, P. Natl. Acad. Sci. USA, 110, 4309–4314, 2013.
Zhang, J. G., Hu, B. H., Ruan, H., and Fang, Y. M.: The present situation and control measures of soil and water loss in Changjiang River valley, Journal of Nanjing Forestry University, 23, 17–21, 1999 (in Chinese with English abstract).
Zhang, P., Shao, G., Zhao, G., Le Master, D. C., Parker, G. R., Dunning, J. B., and Li, Q.: China's forest policy for the 21st century, Science, 288, 2135–2136, 2000.

Table 1. Characteristics of hydro-meteorological stations in the Kejie watershed.

Site Name	Latitude	Longitude	Elevation (m)	Period	Type
Baoshan	25°07′	99°11′	1652	1965–2010	Meteorological
Changning	24°49′41″	99°37′12″	1658	1965–2010	Stations with
Ganwangkeng	25°13′32	99°09′41″	1955	1998–2002	6 parameters
Shidian	24°43′51″	99°11′00″	1489	1965–2010	
Beimiaoshuiku	25°14′47″	99°12′38″	1730	1965–2005	Rainfall
Damaidi	25°15′11″	99°08′02″	2225	1998–2002	Stations
Dawopo	25°13′37″	99°09′11″	2120	1998–2002	
Kejie	24°52′50″	99°25′36″	968	1965–2005	
Laishitou	25°15′58″	99°07′08″	3076	1998–2002	
Lijiasi	25°14′35″	99°09′07″	1970	1998–2002	
Qingshui	25°13′54″	99°10′17″	1852	1998–2002	
Shangoushui	25°15′00″	99°09′04″	2090	1998–2002	
Xizhuang	25°13′08″	99°12′22″	1705	1998–2002	
Kejie	24°52′50″	99°25′36″	968	1965–2010	Hydrological station
Baimiaoshuiku	25°14′47″	99°12′38″	1730	1965–2010	Reservoir outflow

HESSD
10, 12417–12451, 2013

Table 2. Mann–Kendall trend tests of *P*, R-factor, Runoff and SS in Kejie watershed; Tau is the Mann–Kendall rank correlation coefficient.

Type	Recorded year	Tau	2-sided value
P	1971–2010	−0.087	0.43503
R-factor	1971–2010	−0.079	0.47726
Runoff	1971–2010	−0.151	0.17283
SS	1971–2010	−0.459	*0.00003*

Note: *P* = annual rainfall; R-factor = rainfall erosivity;
SS = suspended sediment

HESSD
10, 12417–12451, 2013

Table 3. Statistics of land-cover area in percent in the Kejie watershed (%).

Type	1974	1991	2001	2006	2009
Forest	21.9	34.5	37.3	44.3	55.8
Grassland	28.1	24.5	17.0	12.7	3.4
Cropland	27.0	23.7	26.0	20.4	32.0
Settlement	3.3	3.5	4.2	5.8	5.3
Barren land	18.9	13.1	14.7	16.2	2.9
Water	0.8	0.8	0.9	0.6	0.5

HESSD
10, 12417–12451, 2013

Table 4. The contribution of ecological and engineering measures to soil loss reduction at 4 plot sites (2000–2005).

Measures		Contribution to soil loss reduction %			
		No1	No2	No3	No4
Ecological measures	soil and water conservation forest	47.5	27.3	35.4	37.0
	economical forest-fruit	1.7	1.1	5.1	7.3
	closed treatment	24.2	12.0	3.6	8.3
	conservative tillage	6.7	5.5	3.6	4.2
Engineering measures	Terrace	15.0	5.5	4.4	5.2
	silt check dam	5.0	48.6	47.8	38.0

Notes: No1 = Ajiadahe basin; No2 = Binmawahe basin; No3 = Santaizihe Basin; No4 = Wadudahe basin.

HESSD
10, 12417–12451, 2013
Reduction of suspended sediment in southwest China
X. Ma et al.

Table 5. The potential disposal of excavated soil and investment in soil and water conservation in construction projects (2004–2010).

Year	Protect area (ha)	Waste soil (10^4 m^3)	Investment on soil and water conservation (10^4 RMB)
2004	8.7	6.5	16.2
2005	15.0	1.1	154.5
2006	38.8	11.4	576.6
2007	1267.9	1607.3	203.6
2008	7.6	91.8	3.0
2009	4.9	1.6	51.2
2010	372.6	187.7	1773.0
Sum	1715.5	1907.3	2778.1

HESSD
10, 12417–12451, 2013

Table 6. The SWAT sediment sensitive parameters and fitted values.

Parameters	Description	fitted values
USLE_P[Forest]	USLE practice factor	0.19
USLE_P[Grassland]	USLE practice factor	0.3
USLE_P[Cropland]	USLE practice factor	0.5
USLE_P[Settlement]	USLE practice factor	0.1
USLE_P[Barren land]	USLE practice factor	0.6
ADJ_PKR.bsn	Peak rate adjustment factor for sediment routing in sub-basin	0.7
SPCON.bsn	Linear re-entrainment parameters for channel sediment routing	0.001
CH_EROD.rte	Channel erodibility factor	0.3

Table 7. Simulated and measured annual suspended sediment yield in the Kejie watershed (1970–2010).

Measured and simulated scenarios			Mean annual SSY ($10^4\ \mathrm{t\,yr^{-1}}$)
Measured 1	Period1	1971–1985	240.8
Measured 2	Period2	1986–2010	145.2
SimulatedL1C1	Period1	1971–1985	237.0
	Land use	Lus1974	
SimulatedL1C2	Period2	1986–2010	213.1
	Land use	Lus1974	
SimulatedL2C2	Period2	1986–2010	169.0
	Land use	Lus1991 + lus2001 + lus2006 + lus2009	

HESSD
10, 12417–12451, 2013

Table 8. Contribution of vegetation restoration, climate change and other engineering measures to suspended sediment between period 1 and 2 in the Kejie watershed.

		Change of annual SSY ($10^4\,t\,yr^{-1}$)	%
Observed change	Measured2 – Measured1	−95.6	
Climate effects	SimulatedL1C2 – SimulatedL1C1	−23.9	25
Land use change effects	SimulatedL2C2 – SimulatedL1C2	−44.1	46
Engineering effects	Measured2 – SimulatedL2C2	−23.8	25
Model Bias	SimulatedL1C1 – Measured1	−3.8	4

HESSD
10, 12417–12451, 2013

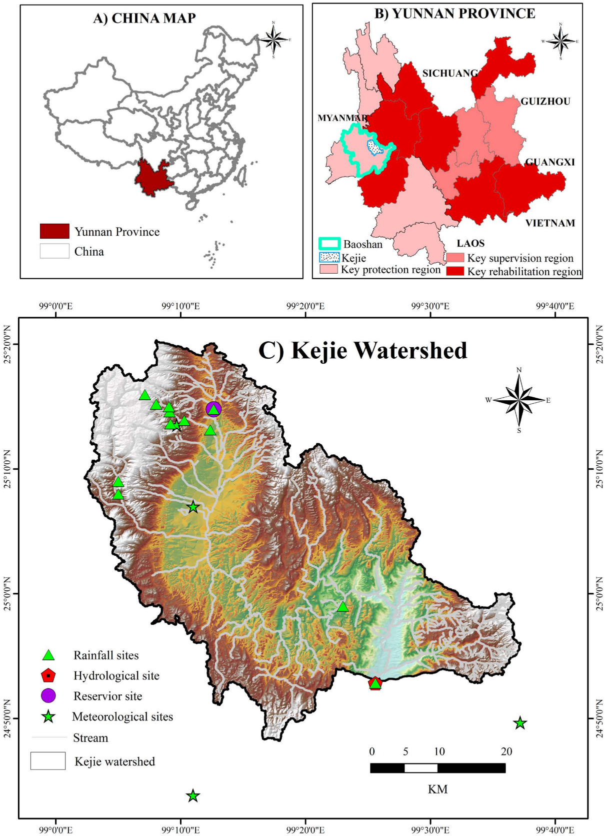

Fig. 1. Location map of the Kejie watershed, Southwest China, with current erosion classification of the province **(B)** and location of weather and rainfall stations plus catchment outflow **(C)**.

HESSD
10, 12417–12451, 2013

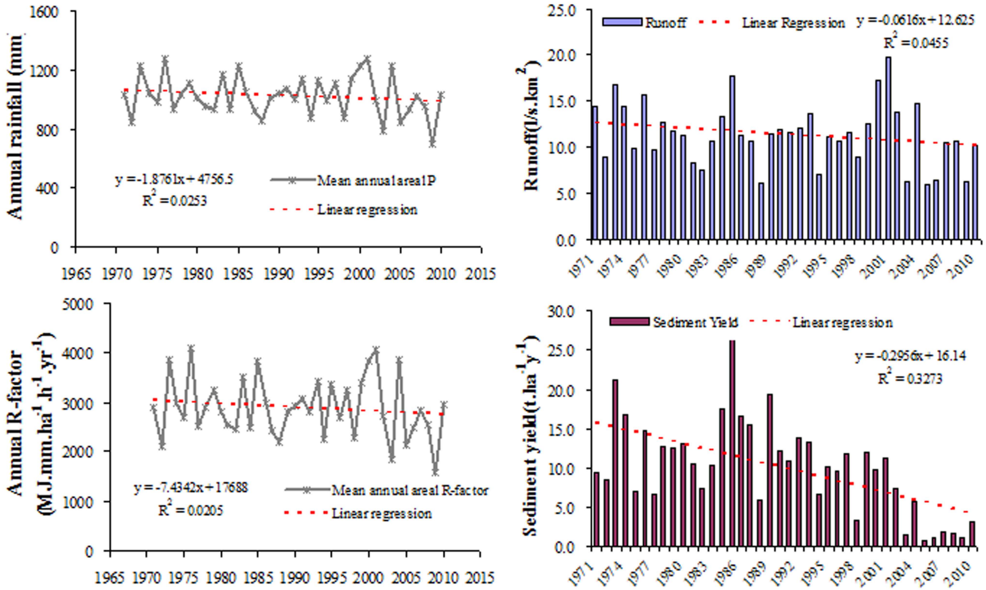

Fig. 2. The trend of areal annual rainfall, rainfall erosivity (R-factor), runoff and sediment yield in the Kejie watershed over 1971–2010.

HESSD
10, 12417–12451, 2013

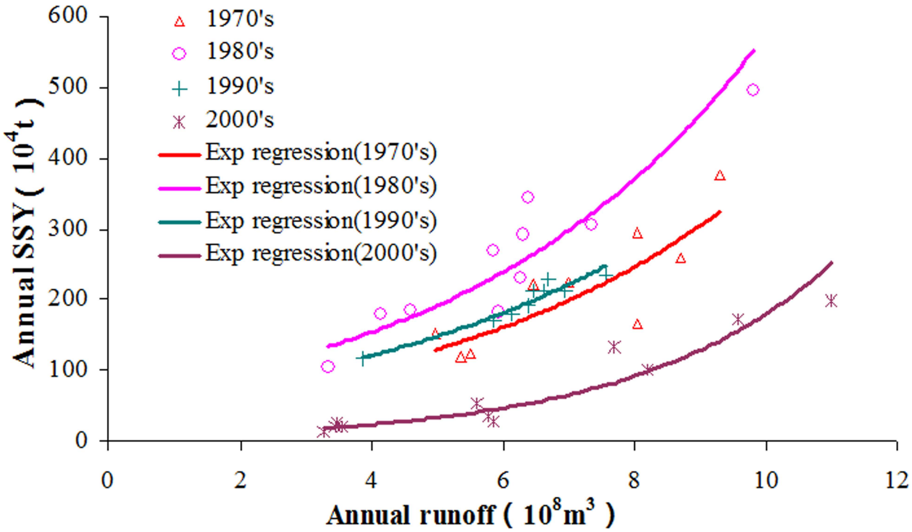

Fig. 3. The relationship between annual runoff and suspended sediment yield in the outlet of the Kejie watershed (1971–2010).

HESSD
10, 12417–12451, 2013

HESSD
10, 12417–12451, 2013

Reduction of suspended sediment in southwest China

X. Ma et al.

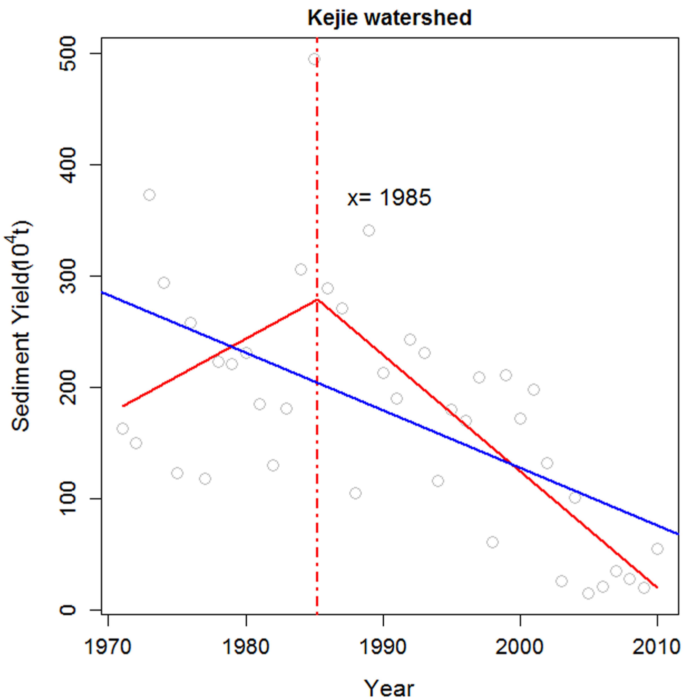

Fig. 4. Change trend of suspended sediment yield in the Kejie watershed from 1965 to 2010 (Red solid lines are the piecewise-regression lines, the blue solid line is the linear regression line, the red dash line is to illustrate the breakpoint).

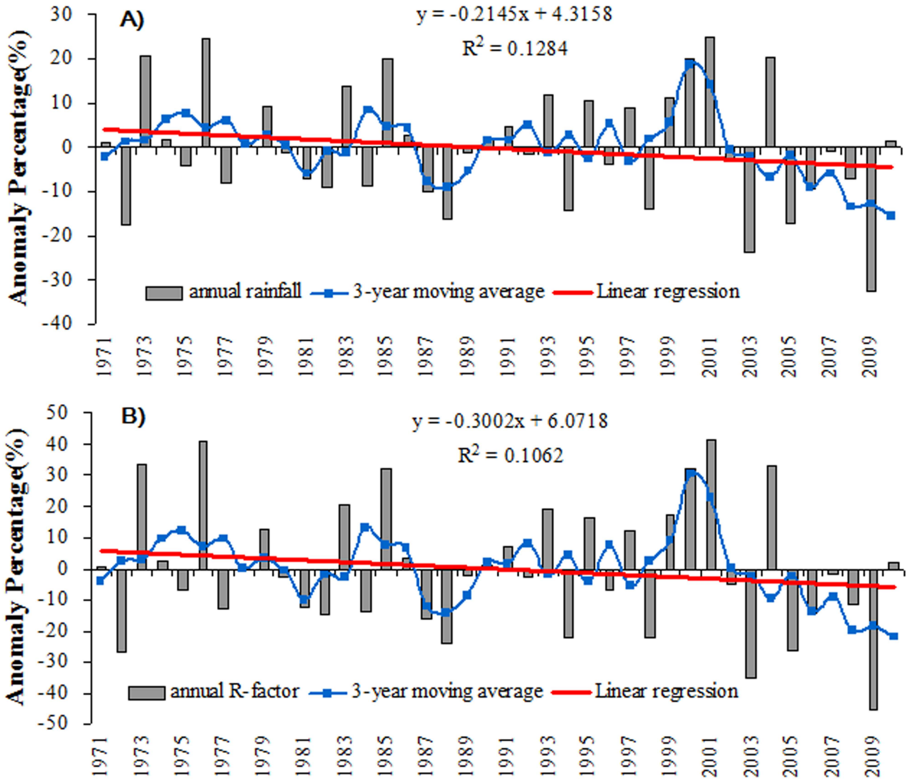

Fig. 5. The inter-annual variability of rainfall and R-factor in the Kejie watershed (1971–2010).

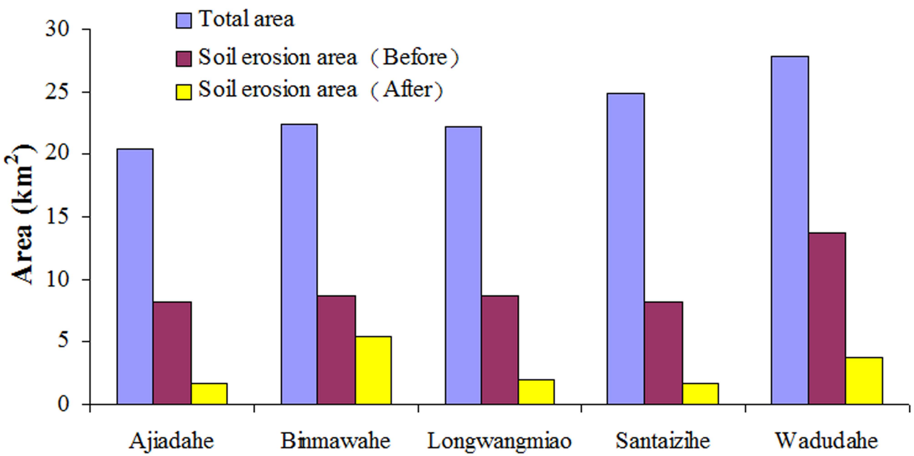

Fig. 6. Soil erosion area before and after soil and water conservation measures implemented at the 5 pilot sites in the Kejie watershed.

HESSD
10, 12417–12451, 2013

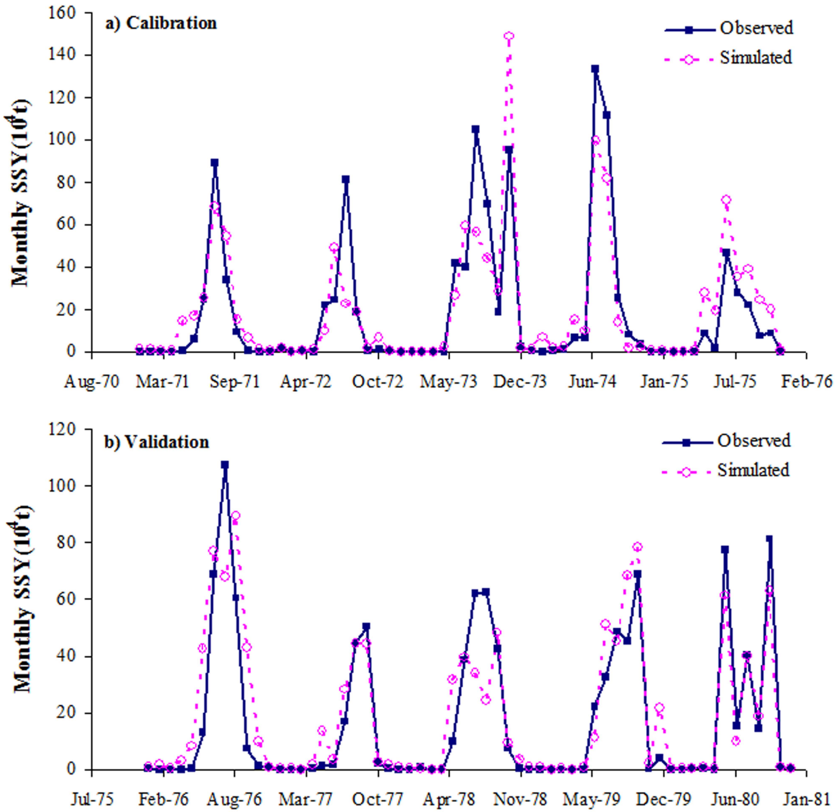

Fig. 7. Mean monthly simulated and observed suspended sediment yield at the outlet of the Kejie watershed for **(a)** the calibration period and **(b)** the validation period.

HESSD
10, 12417–12451, 2013
Reduction of suspended sediment in southwest China
X. Ma et al.

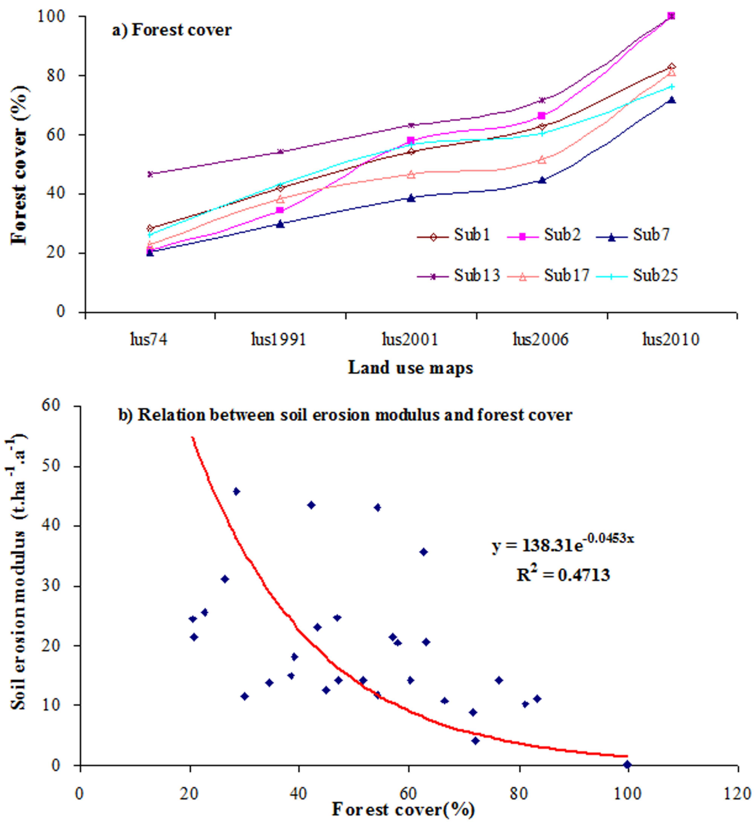

Fig. 8. Relationship between forest cover and soil erosion modulus at the 6 sub-basins **(b)** with similar forest cover change trend **(a)** in the Kejie watershed from 1974 to 2010.

HESSD
10, 12417–12451, 2013

Reduction of suspended sediment in southwest China

X. Ma et al.